

# PyJama: Differentiable Jamming and Anti-Jamming with NVIDIA Sionna

Fabian Ulbricht, Gian Marti, Reinhard Wiesmayr, and Christoph Studer

*Department of Information Technology and Electrical Engineering, ETH Zurich, Switzerland  
email: fabianu@student.ethz.ch, marti@iis.ee.ethz.ch, wiesmayr@iis.ee.ethz.ch, studer@ethz.ch*

**Abstract**—Despite extensive research on jamming attacks on wireless communication systems, the potential of machine learning for amplifying the threat of such attacks, or our ability to mitigate them, remains largely untapped. A key obstacle to such research has been the absence of a suitable framework. To resolve this obstacle, we release PyJama, a fully-differentiable open-source library that adds jamming and anti-jamming functionality to NVIDIA Sionna. We demonstrate the utility of PyJama (i) for realistic MIMO simulations by showing examples that involve forward error correction, OFDM waveforms in time and frequency, realistic channel models, and mobility; and (ii) for learning to jam. Specifically, we use stochastic gradient descent to optimize jamming power allocation over an OFDM resource grid. The learned strategies are non-trivial, intelligible, and effective.

## I. INTRODUCTION

Jamming attacks on wireless communication systems are a growing concern and have been studied extensively [1]. Since machine learning (ML) had a transformative impact on communication engineering [2], [3], it might be expected to enhance our understanding of jamming attacks and facilitate new ways of mitigating such attacks. However, the potential of ML for either jamming or anti-jamming remains largely untapped, mainly due to the lack of a suitable framework.

### A. Contributions

In order to facilitate the use of ML for research in jamming and anti-jamming, we release PyJama, a fully-differentiable open-source library that adds jamming and anti-jamming (with a focus on MIMO anti-jamming) functionality to NVIDIA Sionna [4]. The combination of Sionna and PyJama enables realistic link-level simulations of wireless communication systems under jamming attacks, including aspects such as jammer-mitigating or jammer-oblivious MIMO receivers; forward error correction (FEC); orthogonal-frequency division multiplexing (OFDM) waveforms in the time or frequency domains; geometric channel models [5]; transmitter, receiver, and jammer mobility; and much more. In Sec. II, we provide a brief overview of PyJama’s application programming interface (API) and showcase some of its capabilities via simulation examples. Extensive documentation and Jupyter notebooks

The work of GM, RW, and CS was supported in part by an ETH Zurich Research Grant.

The authors thank J. Hoydis, S. Cammerer, and F. A. Aoudia for comments and discussions on NVIDIA Sionna. The authors also thank C. Dick for helpful comments and discussions.



for all of our experiments are available on `pyjama.ethz.ch`. We then leverage PyJama for learning to jam (against traditional receivers as well as against basic anti-jamming MIMO receivers), by using stochastic gradient descent to optimize jamming power allocation over an OFDM resource grid. We also propose suitable jammer loss functions for uncoded and coded communication systems. The learned jamming strategies are nontrivial, intelligible, and highly effective.

### B. Prior Work

Prior studies on jamming and anti-jamming strategies have often used game-theoretic approaches, where transmitters and jammers correspond to actors in Bayesian games [6] or Stackelberg games [7], [8] that model basic communication schemes. Other studies have used reinforcement learning (RL), such as Q-learning [9]–[11], bandit optimization [12], or adversarial ML [3], [13]. All these works rely on basic models for the received signal-to-interference-plus-noise ratio (SINR) and are unable to account for the specifics of real-world communication systems such as waveforms, channel coding, etc.

Spatial filtering has recently gained traction as a powerful tool for jammer mitigation in MIMO systems [1], but it is known that smart jammers can evade simple mitigation schemes at the receiver [14]. While [8], [11], [12] consider jamming in MIMO systems, they do not leverage ML for learning adversarial jamming strategies against MIMO anti-jamming receivers, making our work the first to do so.

### C. Prerequisites

PyJama is designed with a focus on MIMO (anti-)jamming. A jammed MIMO communication system can be modeled in discrete time as

$$\mathbf{y}[k] = \sum_{\ell=0}^{L-1} (\mathbf{H}[k, \ell] \mathbf{s}[k - \ell] + \mathbf{J}[k, \ell] \mathbf{w}[k - \ell]) + \mathbf{n}[k], \quad (1)$$

where  $\mathbf{y}[k] \in \mathbb{C}^B$  is the time- $k$  receive signal at a  $B$ -antenna receiver;  $\mathbf{s}[k] \in \mathbb{C}^U$  and  $\mathbf{w}[k] \in \mathbb{C}^I$  are the time- $k$  transmit signals at one or multiple transmitters and one or multiple jammers with a total of  $U$  and  $I$  antennas, respectively;  $\mathbf{H}[k, \ell] \in \mathbb{C}^{B \times U}$  and  $\mathbf{J}[k, \ell] \in \mathbb{C}^{B \times I}$  represent the impulse response matrices at time  $k$  and delay  $\ell < L$  of the transmitter and jammer channels, respectively; and  $\mathbf{n}[k] \in \mathbb{C}^B$  is white Gaussian noise. In flat fading systems, the input-output relation in (1) can be simplified to  $\mathbf{y}[k] = \mathbf{H} \mathbf{s}[k] + \mathbf{J} \mathbf{w}[k] + \mathbf{n}[k]$ .

A receiver that uses a conventional data detector, such as an LMMSE equalizer without any anti-jamming capability, will experience significantly increased error rates under jamming. In contrast, an anti-jamming receiver can mitigate the jamming interference through spatial filtering, for instance by projecting the receive signal onto the orthogonal complement of the jammer’s subspace (“POS”) to null the jammer,<sup>1</sup> or by using an LMMSE equalizer that treats the jammer interference as spatially correlated noise (“IAN-LMMSE”) [15].

## II. PYJAMA: API AND EXAMPLES

We release PyJama, a TensorFlow-based open-source library that adds fully differentiable jamming and MIMO anti-jamming functionality to NVIDIA Sionna [4]. The library, extensive API documentation, tutorials, and simulation code to reproduce the results of this paper are available on `pyjama.ethz.ch`.

### A. API Overview

Fig. 1 shows a basic PyJama-Sionna simulation pipeline of a coded OFDM system (forked arrows indicate multiple options).

1) *Jammers*: PyJama enables the simulation of jammed communication systems in the time as well as frequency domain. Frequency-domain simulations are computationally more efficient while time-domain simulations can account for effects that are otherwise ignored, such as MIMO-OFDM jammers that do not transmit a cyclic prefix (see Sec. II-B3). In both domains, jammers are implemented as communication blocks that superimpose the jamming interference on the output of an unjammed wireless channel (see Fig. 1). This approach enables the use of potentially different channel models for the jammers and the transmitters (see Sec. II-B2). PyJama features jammers that transmit symbols drawn uniformly from a complex disk, complex Gaussian symbols, symbols from a QAM constellation, or symbols provided by a Python callable (see Fig. 2). While time-domain jammers currently only support barrage (i.e., stationary) jamming, frequency-domain jammers can be configured as barrage jammers, pilot jammers, data jammers, or sparse (in time or frequency) jammers (see Fig. 2).

2) *Receivers*: PyJama implements the two anti-jamming receive methods POS and IAN-LMMSE (see Sec. I-C). While POS can be put in front of any Sionna equalizer, IAN-LMMSE unifies jammer mitigation and data detection, and so is a complete equalizer by itself (see Fig. 1). POS and IAN-LMMSE can either operate using perfect channel state information (CSI) for the transmitters and the jammers, or they can estimate the CSI (which requires new pilot patterns for jammer estimation; see below). For learning in coded systems—not necessarily restricted to (anti-)jamming applications—PyJama also implements an iteration-loss LDPC decoder (see Fig. 1).

3) *Transmitters*: In real-world wireless systems, CSI has to be obtained through channel estimation. Since the anti-jamming receivers of PyJama depend on the jammers’ CSI, PyJama implements the `PilotPatternWithSilence`, which is a wrapper for a Sionna pilot pattern that adds “silent” resource

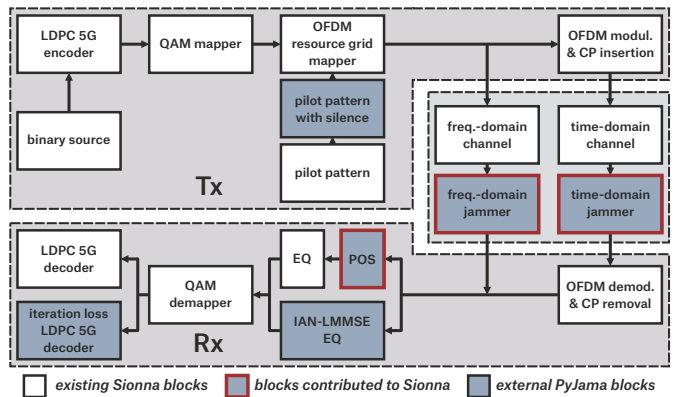


Fig. 1. PyJama simulation pipeline (channel estimation not shown). In Sionna, the frequency-domain and time-domain jammers are implemented as (generalized) frequency-domain and time-domain interference classes, respectively.

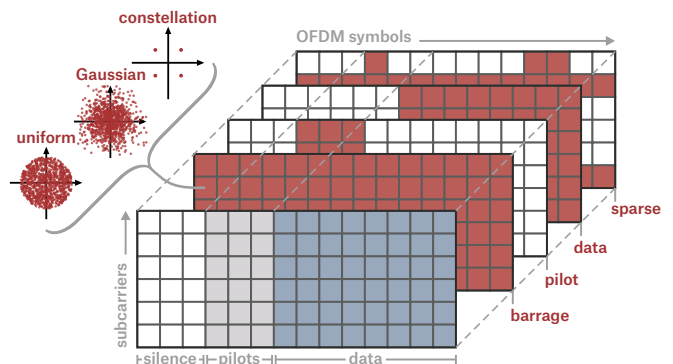


Fig. 2. Foreground: Illustration of an OFDM resource grid that uses the `PilotPatternWithSilence`. Background: Corresponding illustration of the different types of frequency domain jammers (barrage jammer, pilot jammer, data jammer, sparse jammer). The jammer transmit symbols can be drawn from a uniform distribution, a Gaussian distribution, or a QAM constellation.

elements (REs) to an OFDM resource grid (cf. Fig. 2). During such silent REs, the transmitters are idle and so enable the receiver to estimate the jammers’ channel matrix up to complex-valued scale factors (provided that the jammers jam these REs).

### B. Examples

Since PyJama builds on Sionna, it enables convenient, fast, and realistic simulation of (potentially anti-jamming) communication systems under jamming attacks. In the following examples, we showcase just a handful of possibilities. All of the included examples consider the uplink of a 5G NR-like multiuser (MU) MIMO system. Unless stated otherwise, the simulations use a 3GPP urban micro (UMi) channel model for both the user equipments (UEs) as well as the jammers. The basestation (BS) has a dual-polarized uniform linear array (ULA) with a total of 16 antennas. We consider four single-polarized single-antenna UEs (with perfect power control) and one single-polarized single-antenna jammer. We use OFDM at a 3.5 GHz carrier frequency and 128 consecutive subcarriers spaced at 30 kHz. The resource grid contains 14 OFDM symbols. For each subcarrier, the first 4 of these symbols are silent (for jammer CSI estimation), the subsequent four symbols contain one-hot pilots (for UE CSI estimation), and

<sup>1</sup>In the flat-fading case, the corresponding projection matrix is  $\mathbf{I}_B - \mathbf{J}\mathbf{J}^\dagger$ .

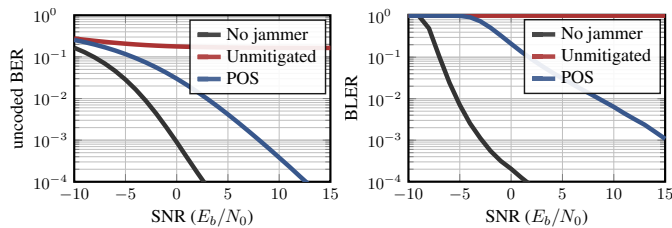


Fig. 3. Left: Uncoded bit error rates (BERs) vs. SNR for basic MIMO jamming and anti-jamming. Right: Corresponding block error rates (BLERs).

the remaining six symbols contain QPSK data symbols. The jammer is a barrage jammer that transmits i.i.d. uniformly sampled symbols from the complex disk. In our experiments, if the receiver uses anti-jamming, then it does so by using POS (see Sec. I-C) in combination with a least-squares (LS) channel estimator and an LMMSE data detector; otherwise, the receiver uses conventional LS channel estimation and LMMSE data detection. In coded simulations, we use a 5G rate-1/2 LDPC code with a block length of 1536 bits, where the decoder uses max-product decoding with 20 flooding iterations.

1) *Bit Error Rate (BER) and Block Error Rate (BLER) Simulations:* Our first example consists of basic BER and BLER simulations (as a function of signal-to-noise ratio  $E_b/N_0$ ) that compare the performance between (i) a conventional receiver that is not attacked by jamming, (ii) a conventional receiver attacked by two 2-antenna jammers that jam at twice the power of the average UE, and (iii) a POS anti-jamming receiver. Fig. 3 shows that the unjammed system has the best performance, while the jammed system with unmitigated receiver suffers from a high error floor that cannot be remedied by the LDPC code (in fact, the BLER is equal to one). The anti-jamming receiver is able to mitigate the jammer and resolve the error floor. The performance loss compared to the unjammed system is due to imperfectly estimated jammer CSI and the loss of four degrees of freedom incurred by the POS projection.

2) *Transmitter and Jammer Mobility:* Studies on MIMO jammer mitigation usually operate, at least implicitly, with a block fading channel model, so that a CSI estimate from some point in time remains valid for a certain period. However, real-world wireless channels are not block fading. In Fig. 4, we use PyJama to evaluate the impact of jammer and UE mobility, which models continually evolving communication channels, on MIMO anti-jamming against a single-antenna jammer that jams at 20 dB higher power than the average UE. The results show that, at low velocities, the impact of UE mobility is negligible while the impact of jammer mobility is not. At high velocities, UE mobility becomes a problem as well, but it is not as critical as jammer mobility.

3) *Time-Domain OFDM Jamming:* In our third example, we simulate a single-antenna OFDM-MIMO jammer (and its mitigation) in the time domain. It has recently been shown [16] that a jammer that violates the OFDM protocol by not transmitting a cyclic prefix (CP) appears on each received subcarrier as high-rank interference—and not as rank-one interference, as an OFDM compliant jammer theoretically would. Specifically, [16] has shown that the rank of the receive

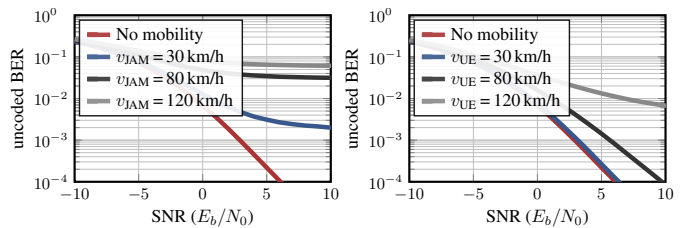


Fig. 4. Left: POS mitigation effectiveness for different levels of jammer mobility. Right: POS mitigation effectiveness for different levels of UE mobility.

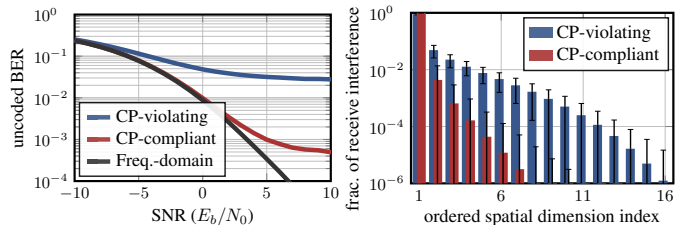


Fig. 5. Left: Error rates of CP-compliant and CP-violating single-antenna jammers under one-dimensional POS mitigation. Right: Normalized histogram of the fraction of receive interference per spatial dimension (in descending order); the jammer simulated in the frequency domain is not shown.

interference per subcarrier for a CP-violating jammer can be up to  $\min\{B, L\}$ , where  $B$  is the number of receive antennas, and  $L$  is the jammer’s number of channel taps in the time domain. Consequently, such jammers cannot be completely mitigated by nulling a single spatial dimension. So far, however, this effect has only been verified on simplistic channel models with i.i.d. Rayleigh fading channel taps, and its impact in more realistic models has not been investigated.

In Fig. 5, we simulate such a scenario. We consider a channel with 20 MHz bandwidth and 30 kHz subcarrier spacing (= 667 subcarriers); the CP-length is  $2.35 \mu\text{s}$  (= 47 channel taps). The left plot shows the error rate for a POS receiver that nulls the strongest spatial interference dimension (based on perfect CSI) for (i) a CP-violating single-antenna jammer simulated in the time domain, (ii) a CP-compliant single-antenna jammer simulated in the time domain, and (iii) a single-antenna jammer simulated in the frequency domain. All jammers jam at 20 dB higher power than the average UE. The results show that, for the first jammer, the receive interference is not restricted to a one-dimensional subspace, which leads to poor performance even after nulling the strongest interference dimension. The frequency-domain simulation ignores effects related to imperfect CPs and so the single-antenna jammer is perfectly nulled by the POS receiver, since it only causes rank-one interference per subcarrier. In theory, if the CP is not shorter than the channel’s impulse response, the CP-compliant jammer should behave identically to the frequency-domain simulation. However, the error floor induced by the CP-compliant jammer indicates that, at least in some cases, the delay spread exceeds the CP length. The right plot in Fig. 5 supports these conclusions by showing normalized histograms of the ordered singular values of the receive jammer interference, which correspond to the relative fraction of receive interference per spatial dimension: A CP-compliant single-

antenna jammer would theoretically cause rank-one interference and thus have only one singular value with non-zero distribution. But we see that the CP-violating jammer has 16 singular values with non-zero distribution, indicating full-rank receive interference (since the BS has only 16 antennas). Even the CP-compliant jammer has multiple singular values with non-zero distribution since the channel impulse response length sometimes exceeds the CP-length. The jammer simulated in the frequency domain is only rank one, and that rank's fraction of receive interference is equal to one (not shown in Fig. 5).

### III. LEARNING TO JAM

While PyJama is equally suited for learning to mitigate jammers, we now use it for *learning to jam*, with the goal of improving our understanding of effective jamming attacks. Specifically, our goal is to learn jammers that maximize the error rate for a given power budget  $\rho_{\max}$  (compared to the average UE), against traditional MIMO receivers as well as POS-based anti-jamming. To this end, we use empirical risk minimization (ERM) based on stochastic gradient descent.

#### A. Fundamentals of Jammer Learning

In order to learn how to jam, one needs a parametrized class of jamming strategies and a model that is differentiable with respect to the parameters of that class. In our case, the jamming strategies are parametrized by a vector  $\boldsymbol{\rho}$  that parametrizes the jamming power allocation (see Sec. III-B); and the model is a PyJama pipeline (as in Fig. 1) simulating a jammed communication system, combined with a loss function  $\ell$  that captures the empirical error. Specifically, PyJama simulates the transmission of information bits  $\mathbf{b} \in \{0, 1\}^N$  with corresponding soft-output estimates  $\hat{\mathbf{b}} \in [0, 1]^N$  at the receiver.<sup>2</sup> The function  $\ell(\mathbf{b}, \hat{\mathbf{b}})$  measures the error between the true bits  $\mathbf{b}$  and their estimates  $\hat{\mathbf{b}}$ . Due to PyJama's differentiability,  $\ell(\mathbf{b}, \hat{\mathbf{b}})$  is differentiable with respect to  $\boldsymbol{\rho}$  as long as it is differentiable with respect to  $\hat{\mathbf{b}}$ . By defining the jammer power allocation vector  $\boldsymbol{\rho}$  as a trainable TensorFlow variable, one can therefore use TensorFlow's autodiff capabilities to learn how to jam.

A commonly used loss function for ML in communications is the binary cross entropy (BCE). While the BCE is well-suited for (bit) error rate *minimization* [17], it is unsuited for error rate *maximization* (which is our goal when learning to jam): The BCE loss  $\ell_{\text{BCE}}(\mathbf{b}, \hat{\mathbf{b}})$  is unbounded on  $\{0, 1\}^N \times [0, 1]^N$  and—in particular—can be arbitrarily large even when only one bit estimate is incorrect, meaning that BCE fails to capture the *rate* of errors. This defect is avoided by loss functions such as the L1 loss and the mean squared error (MSE); see Tbl. I. Both of these have proven to work well for the task at hand.

#### B. Training Model

We simulate a MU-MIMO OFDM system as in Sec. II-B in the frequency domain, with the following differences: (i) depending on the experiment, the number of UEs (and the

<sup>2</sup>The soft-outputs  $\hat{\mathbf{b}} = (\hat{b}_1, \dots, \hat{b}_N) \in [0, 1]^N$  represent bit estimates in the probability domain, not LLRs. Specifically,  $\hat{b}_n$  represents the estimate of the probability  $P(b_n = 1)$  that the  $n$ th transmitted bit is one.

TABLE I  
UNSUITABLE (✗) AND SUITABLE (✓) JAMMER LOSS FUNCTIONS

BCE ✗	L1 ✓	MSE ✓
$-\sum_{n=1}^N \frac{b_n \log \hat{b}_n + (1 - b_n) \log(1 - \hat{b}_n)}{N}$	$\sum_{n=1}^N \frac{ b_n - \hat{b}_n }{N}$	$\sum_{n=1}^N \frac{(b_n - \hat{b}_n)^2}{N}$

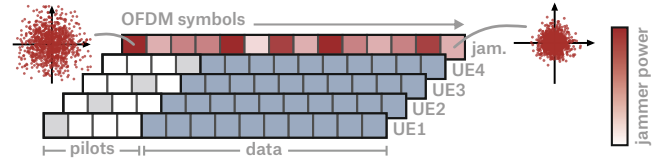


Fig. 6. Illustration of the UE resource grid for a classical MIMO receiver (only one subcarrier shown) with 4 UEs and one-hot pilots, and of a trainable jammer.

corresponding length of the pilots) varies between one and eight; (ii) depending on the experiment, the receiver is either the conventional MIMO receiver (in which case the resource grid contains no silent symbols; see Fig. 6) or the POS receiver from Sec. II-B1; (iii) the jammer transmits independent Gaussian symbols, where the symbols transmitted during the  $i$ th OFDM symbol have trainable power  $\rho_i$  subject to a power constraint  $\|\boldsymbol{\rho}\|_1 / N_s \triangleq \frac{1}{N_s} \sum_{i=1}^{N_s} \rho_i \leq \rho_{\max}$ , where  $N_s = 14$  is the number of OFDM symbols per resource grid; see Fig. 6. When considering uncoded systems, we use the L1 loss from Tbl. I. When considering coded systems (with an LDPC code as described in Sec. II-B), we use an iteration loss LDPC 5G decoder based on the L1 loss of the information bits (cf. Fig. 1), which returns soft estimates of the information bits after every iteration, and which we use as a multi-loss function [18].

For optimization, we use Adam with a learning rate of  $10^{-3}$ . We train for 5000 gradient steps, each of which processes a batch of 64 transmitted OFDM frames at an SNR of 0 dB.

#### C. Learning Results

1) *Conventional Receiver, Uncoded Communications*: Fig. 7 shows the learned jammer power allocation for different jammer power budgets and different numbers of UEs. The results show that the learned strategy depends heavily on the specific setting.

In single-UE settings, the jammer focuses its energy primarily on the pilot symbol. In few-UE settings, the learned strategies differ depending on the power budget: a weak jammer jams primarily the pilots, but often targets one or two UEs (since one-hot pilots are used, jamming, e.g., the third OFDM symbol affects the channel estimate, and thus the error rate, of the third UE); a strong jammer, in contrast, learns to focus the energy on the data symbols, which affects all UEs equally. Finally, in many-UE settings, the jammer focuses its energy primarily on the data symbols, irrespective of its power budget.

In terms of effectiveness, we note that the learned jammer always outperforms a uniform barrage jammer: at an SNR of 5 dB, the BER for the trained jammer exceeds the BER of an equally strong barrage jammer by factors between 1.00 and 7.19. The effectiveness of jammer learning can also be quantified in terms of a power gain: The left plot in Fig. 8 shows that a learned jammer with a power budget

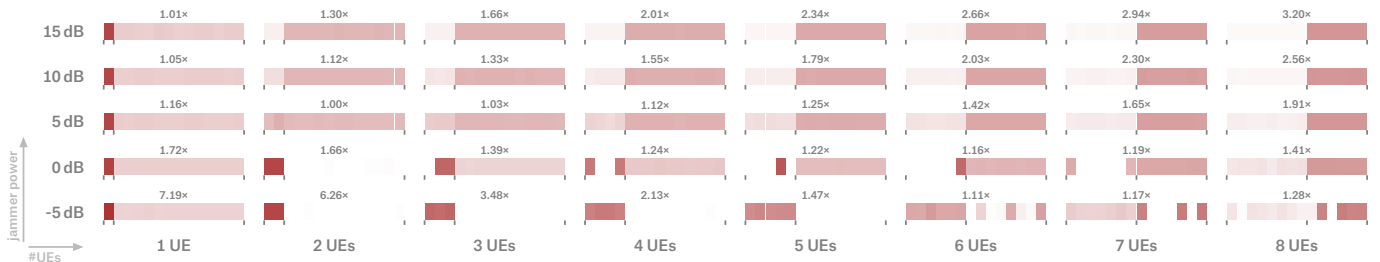


Fig. 7. Learned jammer power allocation for different jammer powers and numbers of UEs. The displayed factors indicate the BER increase at an SNR of 5 dB between the learned jammer and a uniform barrage jammer. The ticks indicate the edges of the pilots (whose lengths equal the number of UEs) and data phases.

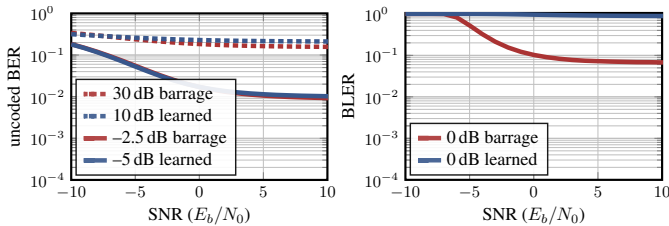


Fig. 8. Performance gains from jammer training against a conventional MIMO receiver with 4 UEs. Left: Jammer powers at which uniform barrage jammers are equally effective (in terms of BER) as learned jammers. Right: BLER against a 0 dB uniform barrage jammer and a 0 dB strong learned jammer.

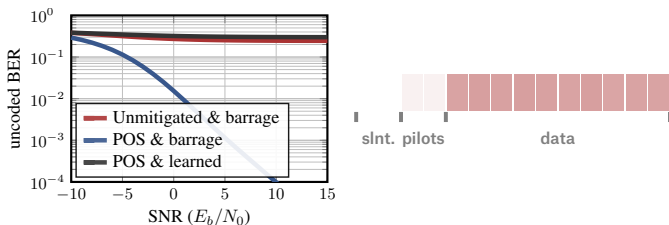


Fig. 9. Performance gains from jammer training against a POS anti-jamming receiver with 4 UEs (left) and learned power allocation that does not jam during the silent symbols (right).

of  $\rho_{\max} = -5$  dB is as effective as a barrage jammer with a power of  $-2.5$  dB, indicating an “effectiveness gain” of 2.5 dB. Moreover, a learned jammer with  $\rho_{\max} = 10$  dB is more effective than a barrage jammer with a power of 30 dB, indicating an improvement of more than 20 dB.

2) *Conventional Receiver, Coded Communications:* The right plot in Fig. 8 shows that learning also improves the effectiveness of jamming against coded systems: while a barrage jammer with 0 dB power only causes a BLER of around 7% (at an SNR of 5 dB), a learned jammer with 0 dB power constraint can drive the BLER up to 90% at the same SNR and, therefore, drive the throughput to almost zero.

3) *POS Anti-Jamming Receiver, Uncoded Communications:* Finally, Fig. 9 show that jammers can learn how to bypass simple mitigation schemes. Here, we consider a POS anti-jamming receiver that estimates the jammer CSI from two silent symbols at the start of the resource grid. The right side of Fig. 9 shows that the jammer learns to simply stay silent during those samples. Then, the POS receiver’s estimate of the jammer CSI consist only of thermal noise, making anti-jamming completely ineffective (see the left side of Fig. 9).

#### IV. CONCLUSIONS AND FUTURE WORK

To unleash the potential of ML for understanding and mitigating jamming attacks, we have presented PyJama, a TensorFlow-based library that adds jamming and (MIMO) anti-jamming capability to NVIDIA Sionna. Together with Sionna, PyJama enables realistic and fully-differentiable link-level simulations of wireless communication systems under jamming attacks.

We have leveraged PyJama to learn optimal jamming strategies in uncoded and coded MIMO-OFDM systems, both against conventional receivers as well as against anti-jamming receivers. The learned jamming strategies are intelligible and highly effective. In particular, the jammers can learn to bypass simple MIMO mitigation schemes—this highlights the need for more sophisticated mitigation strategies.

#### REFERENCES

- [1] H. Pirayesh and H. Zeng, “Jamming attacks and anti-jamming strategies in wireless networks: A comprehensive survey,” *IEEE Commun. Surveys Tuts.*, 2022.
- [2] T. O’Shea and J. Hoydis, “An introduction to deep learning for the physical layer,” *IEEE Trans. Cogn. Commun. Netw.*, 2017.
- [3] T. Erpek *et al.*, “Deep learning for wireless communications,” *Development and Analysis of Deep Learning Architectures*, 2020.
- [4] J. Hoydis *et al.*, “Sionna: An open-source library for next-generation physical layer research,” *arXiv:2203.11854*, 2022.
- [5] —, “Sionna RT: Differentiable ray tracing for radio propagation modeling,” *arXiv:2303.11103*, 2023.
- [6] Y. Sagduyu *et al.*, “Jamming games in wireless networks with incomplete information,” *IEEE Commun. Mag.*, 2011.
- [7] D. Yang *et al.*, “Coping with a smart jammer in wireless networks: A stackelberg game approach,” *IEEE Trans. Wireless Commun.*, 2013.
- [8] Z. Shen *et al.*, “Beam-domain anti-jamming transmission for downlink massive mimo systems: A stackelberg game perspective,” *IEEE Trans. Inf. Forensics Security*, 2021.
- [9] G. Han *et al.*, “Two-dimensional anti-jamming communication based on deep reinforcement learning,” in *IEEE ICASSP*, 2017.
- [10] X. Liu *et al.*, “Anti-jamming communications using spectrum waterfall: A deep reinforcement learning approach,” *IEEE Commun. Lett.*, 2018.
- [11] L. M. Hoang *et al.*, “Multiple correlated jammers suppression: A deep dueling Q-learning approach,” in *IEEE WCNC*, 2022.
- [12] G. Kim and H. Lim, “Reinforcement learning based beamforming jammer for unknown wireless networks,” *IEEE Access*, 2020.
- [13] T. Erpek *et al.*, “Deep learning for launching and mitigating wireless jamming attacks,” *IEEE Trans. Cogn. Commun. Netw.*, 2018.
- [14] G. Marti *et al.*, “Mitigating smart jammers in multi-user MIMO,” *IEEE Trans. Signal Process.*, 2023.
- [15] G. Marti and C. Studer, “Universal MIMO jammer mitigation via secret temporal subspace embeddings,” in *Asilomar Conf.*, 2023.
- [16] —, “Single-antenna jammers in MIMO-OFDM can resemble multi-antenna jammers,” *IEEE Commun. Lett.*, 2023.
- [17] R. Wiesmayr *et al.*, “Bit error and block error rate training for ML-assisted communication,” in *IEEE ICASSP*, 2023.
- [18] E. Nachmani *et al.*, “Deep learning methods for improved decoding of linear codes,” *IEEE J. Sel. Topics Signal Process.*, 2018.